IEEE Access
Multidisciplinary ⋮ Rapid Review ⋮ Open Access Journal

Received 31 July 2024, accepted 15 August 2024, date of publication 19 August 2024, date of current version 29 August 2024.

Digital Object Identifier 10.1109/ACCESS.2024.3445975

RESEARCH ARTICLE

Two-Dimensional 15/24 Non-Isolated Patterned Modulation Codes With Minimum Hamming Distance 3 in Bit-Patterned Media Recording

THIEN AN NGUYEN AND JAEJIN LEE, (Member, IEEE)
Department of Information Communication Convergence Technology, Soongsil University, Seoul 06978, South Korea

Corresponding author: Jaejin Lee (zlee@ssu.ac.kr)

This work was supported by the National Research Foundation of Korea (NRF) Grant funded by Korean Government (MSIT) under Grant 2021R1A2C1011154.

ABSTRACT Reducing the distance between magnetic islands is essential for increasing the areal density in bit-patterned media recording (BPMR). Consequently, significant two-dimensional (2D) interference emerges, encompassing inter-symbol interference (ISI) and inter-track interference (ITI) along the cross- and down-tracks, respectively. To address the 2D interference, modulation with non-isolated patterns can be employed to mitigate the interference from neighboring bits. In previous studies, authors relied on the Hamming code to propose a non-isolated modulation code with a minimum Hamming distance (MHD) of 3. However, for encoding, authors utilized a mapping method with a large look-up table, resulting in prolonged delay for the decoder. Therefore, in this paper, we proposed a generator matrix for creating the Hamming code with an MHD of 3, thereby generating reverse codewords in the look-up table. Consequently, only half of the look-up table needs to be stored, leading to reduced complexity and delay time in the decoder for non-isolated modulation code with an MHD of 3. Simulation results demonstrate that our proposed model can enhance bit error rate performance and decrease delay time compared to previous studies.

INDEX TERMS Bit-patterned media recording (BPMR), error correction codes (ECCs), Hamming code, modulation coding, non-isolated pattern.

I. INTRODUCTION

Bit-patterned media recording (BPMR) emerges as a promising frontier in the evolution of magnetic storage technology. In this innovative approach, data is stored within the magnetic poles of islands [1]. However, as we seek to enhance areal density (AD) by reducing the distance between these islands, a significant challenge arises two-dimensional (2D) interference. This interference, comprising both inter-symbol interference (ISI) and inter-track interference (ITI) from cross- and down-track interactions respectively, poses a substantial obstacle [2]. To overcome this hurdle, advanced detection techniques and channel coding methods are employed to effectively mitigate and eliminate 2D interference, ensuring optimal storage performance.

For detection methods, the equalizer and generalized partial response (GPR) target [3] are used to convert the received signal to the desired signal and estimate the channel parameters. To apply one-dimensional Viterbi for detection, Cideciyan et al. introduced a partial response maximum likelihood (PRML) detection in [4]. Wang and Kumar designed a hybrid 2D equalizer in [5] based on GPR [3] and the modified Viterbi algorithm [6]. Recently, with the development of machine learning, Jeong and Lee proposed a soft-output detector using a multi-layer perceptron in [7]. In addition, deep neural networks are used to predict the media noise and provide support for detection in [8].

In channel coding methods, user data undergo modulation into a non-isolated pattern, ensuring consistency between neighboring and targeted islands. This strategic approach effectively minimizes interference originating from adjacent islands, bolstering overall storage performance. Error-correcting 5/6 modulation codes are proposed for regular and staggered BPMR in [9] and [10], respectively. Based on the K-means algorithm, Jeong and Lee designed the modulation

The associate editor coordinating the review of this manuscript and approving it for publication was Faissal El Bouanani.

decoding in [11]. Recently, the combination of a non-isolated pattern and Hamming code is proposed in [12].

However, in [12], the authors employed the mapping method alongside a sizable look-up table for encoding, resulting in prolonged decoding delays. To address this issue, our paper introduces a generator matrix for generating Hamming code with a minimum Hamming distance (MHD) of 3. This generates reverse codewords, effectively halving the size of the required look-up table. Consequently, this innovation significantly reduces both complexity and decoding delay for non-isolated pattern modulation code with an MHD of 3.

Additionally, we compare three types of 15/24 modulation codes with an MHD of 3. One includes codewords with the non-isolated patterns, where each '1' is surrounded by '0' and vice versa. The second incorporates codewords with non-ITI patterns (avoiding ITI and allowing ISI). Finally, the third incorporates codewords with non-ISI patterns (avoiding ISI and allowing ITI). Simulation results demonstrate that our proposed codewords can improve the BER performance of BPMR systems compared to previous studies. Specifically, with the non-ITI patterns, the model can achieve the best performance.

The contributions of this paper are summarized as follows:

- We present a method to create the generator matrix for the reversed codewords with an MHD of 3, thereby reducing half the size of the look-up table.
- We propose a new method for encoding and decoding, which reduces half of the complexity compared to the previous study.
- We create the 15/24 non-isolated codewords with three types: non-isolated, non-ITI (the vertical patterns), and non-ISI (the horizontal patterns).
- We provide simulation results to verify our proposed method.

This paper is organized as follows: In Section II, a channel model for BPMR is introduced. Simultaneously, we present the proposed method in Section III. Section IV analyzes and discusses the simulation results. Finally, the conclusions are given in Section V.

II. BPMR CHANNEL

In our investigation, we utilized a BPMR channel as described in [13]. A 2D pulse response depicts the received signal from the BPMR systems. The user data, represented as $u[k]$ and belonging to the set {0,1} (0 and 1 as the values of bit), are then stored in the medium in a 2D form denoted as $c[j, k]$, where the elements of $c[j, k]$ are drawn from the set {–1,1} (–1 and 1 as the values of magnetic poles).

The readback signal $b[j, k]$ is influenced by 2D interference, track misregistration (TMR), and media noise, as expressed below:

$$b[j,k] = \sum_{m=-1}^{1}\sum_{n=-1}^{1} h[m,n]\, c[j-m, k-n] + w[j,k], \tag{1}$$

where j and k represent discrete indices corresponding to the track position and symbol position within the track, respectively. The term $w[j, k]$ denotes additive white Gaussian noise (AWGN) characterized by a mean of zero and variance of σ^2. The coefficients of the BPMR channel, denoted as $h[m, n]$, are computed based on the channel pulse response as follows:

$$h[m,n] = P\left(mT_x - \Delta_{off}, nT_q\right). \tag{2}$$

The expression $P(x, q)$ represents a 2D Gaussian pulse response, as described in a previous study [14].

$$P(x,q) = \exp\left(-\frac{1}{2}\left[\left(\frac{x+\Delta_x}{\mu PW_x}\right)^2 + \left(\frac{q+\Delta_q}{\mu PW_q}\right)^2\right]\right), \tag{3}$$

where x and q denote the cross- and down-track axes, respectively. The terms PW_x and PW_q denote the pulse width at half maximum (PW_{50}) in the cross- and down-track directions, respectively, with $\mu = 1/2.3548$. The terms T_x and T_q represent the track pitch and bit period, respectively. In this context, Δ_{off} denotes the read-head offset in the track misregistration (TMR) effect and is expressed as follows:

$$\Delta_{off} = \frac{\text{TMR}\,(\%)\, T_x}{100}. \tag{4}$$

Moreover, Δ_x and Δ_q were modeled as correlated Gaussian random processes based on a previous study [14]. White Gaussian noise was generated using a digital filter with the equation $\Delta(t) = \varepsilon\Delta(t-1) + \theta n_w(t)$, where $\varepsilon = 0.9$, $\theta = \sqrt{1-\varepsilon^2}$, n_w represents the input white noise, and Δ corresponds to the value of Δ_x and Δ_q.

III. PROPOSED SCHEME

This section presents the method to create the generator matrix $\mathbf{G}$, aiding the encoder in converting user data to the non-isolated codewords with an MHD of 3. Additionally, this process generates reverse codewords in the look-up table.

Firstly, since the generator matrix $\mathbf{G} = [\mathbf{I}|\mathbf{P}]$, we need to create the parity matrix $\mathbf{P}$. In matrix $\mathbf{P}$, we select binary sequences with a weight greater than two. Simultaneously, the number of '1's is odd in each column. An example of the matrix $\mathbf{P}$ is provided below:

$$\mathbf{P} = \begin{bmatrix} 1 & 1 & 1 & 1 \\ 1 & 0 & 1 & 0 \\ 0 & 1 & 1 & 0 \\ 1 & 1 & 0 & 0 \end{bmatrix}. \tag{5}$$

To calculate the size of the matrix $\mathbf{P}$, we assume that the number of bits of a binary sequence in each row of $\mathbf{P}$ is denoted by s. The number of binary sequences that have a weight greater than one is $2^s - s - 1$. If we sum up these binary sequences, we obtain the binary sequence $000\ldots0$. Therefore, to ensure an odd number of '1's in each column of $\mathbf{P}$, we remove a binary sequence from the aforementioned list, resulting in the number of rows of $\mathbf{P}$ being $r = 2^s - s - 2$.

Here are the steps to create the list of these codewords:

- *Step 1:* Create the generator matrix $\mathbf{G} = [\mathbf{I}|\mathbf{P}]$, where $\mathbf{I}$ is the identity matrix and $\mathbf{P}$ is created as described above.

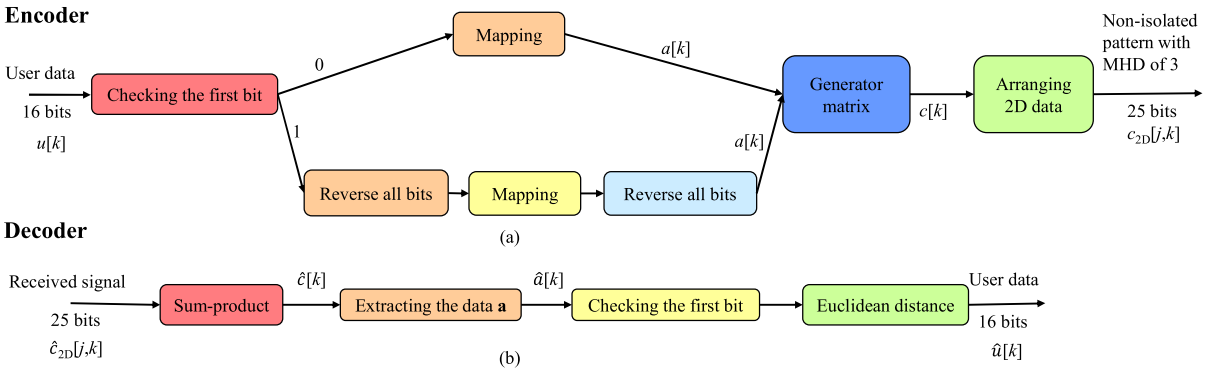

FIGURE 1. Diagram of the proposed (a) encoder and (b) decoder.

- *Step 2:* Generate the Hamming codeword using the following equation.

$$\mathbf{c}^T = \mathbf{a}^T\mathbf{G}, \tag{6}$$

where ^{T} is the transpose operator, $\mathbf{a}$ is a binary vector with the size of $r \times 1$, and $\mathbf{c}$ is a vector of codewords with the size of $v = r + s = 2^s - 2$.

- *Step 3:* Rearrange the vector $\mathbf{c}$ into a 2D form. We estimate a prime factor of v as α. $\mathbf{c}_{2D}$ will have α rows and $\beta = \frac{v}{\alpha}$ columns.
- *Step 4:* Check for the isolated pattern in $\mathbf{c}_{2D}$ using the method described in [12].

After eliminating all the isolated patterns from $\mathbf{c}_{2D}$, we observe that half of the codeword list is the reverse of the other half. Therefore, to create the encoder shown in Fig. 1(a), we only need to store half of the codeword list in the look-up table.

While it is possible to optimize the code rate with $r = 2^s - s - 2$, it is also feasible to remove more than one binary sequence to achieve an odd number of '1's in each column of $\mathbf{P}$, as shown in equation (7)

$$r = 2^s - s - 2\theta - 2 \text{ with } \theta = 0, 1, 2, \ldots \tag{7}$$

In this paper, we consider three types of patterns for codewords: (1) patterns having the same number of columns and rows, (2) patterns having a greater number of rows than columns, and (3) patterns having more columns than rows.

For the first type of the codewords, we choose $s = 5$ and $\theta = 3$. This yields $v = 24$, and arrange the codewords $\mathbf{c}_{2D}$ with a size of 4×6. The non-isolated patterned codes exclude the isolated patterns presented in Fig. 2.

Based on the steps described (1 to 4), we found 37781 non-isolated patterns of $\mathbf{c}_{2D}$. Therefore, the user data $\mathbf{u}$ has $\lfloor \log_2(37781) \rfloor = 15$ bits. We utilize the first bit of $\mathbf{u}$ to split the set of user data into two parts. If the first bit is 0, we assign these binary sequences as the codewords in the look-up table of $\mathbf{c}_{2D}$. If the first bit is 1, we reverse these binary sequences and assign the reversed binary sequences as the codewords in the look-up table. Then, these codewords are reversed again before transmitting to the channel. In Fig. 3, we present randomly selected 10 codewords of 15/24 modulation code with an MHD of 3.

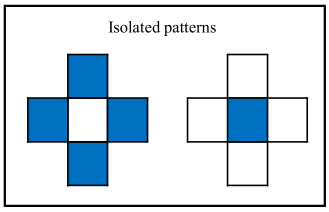

FIGURE 2. Isolated patterns that we want to avoid.

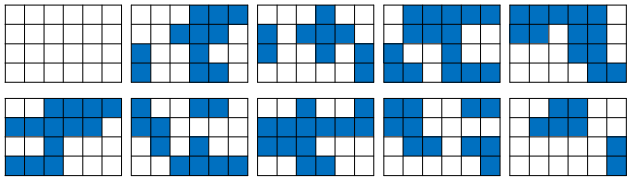

FIGURE 3. 15/24 non-isolated codewords with an MHD of 3.

To decode the received signal, we employ the sum-product algorithm to decode the Hamming code $\hat{c}[k]$. Then, we extract the data $\hat{a}[k]$ from $\hat{c}[k]$. We utilize the first bit to check for reverse sequences. Finally, we compute the Euclidean distance between the signal $\hat{a}[k]$ and the codewords in look-up table to detect the original signal $\hat{u}[k]$. The diagram of decoder is presented in Fig. 1(b).

For the second type of the codewords, we choose $s = 5$ and $\theta = 1$, resulting in $v = 24$ as with the first type. However, we utilize patterns with a size of 8×3. In these patterns, we only avoid ITI (non-ITI patterns) while allowing ISI, as shown in Fig. 4.

We obtained 34341 non-ITI patterns of $\mathbf{c}_{2D}$. Therefore, the user data $\mathbf{u}$ has $\lfloor \log_2(34341) \rfloor = 15$ bits. Here are 10 randomly selected non-ITI patterns presented in Fig. 5.

For the third type of the codewords, we again choose $s = 5$ and $\theta = 1$, resulting in $v = 24$ as with the first and

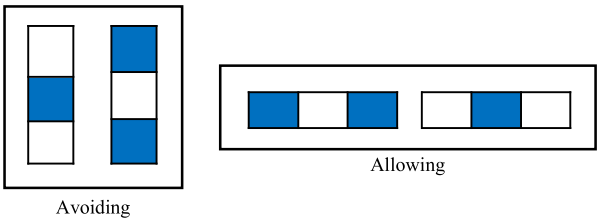

FIGURE 4. ITI patterns that we want to avoid.

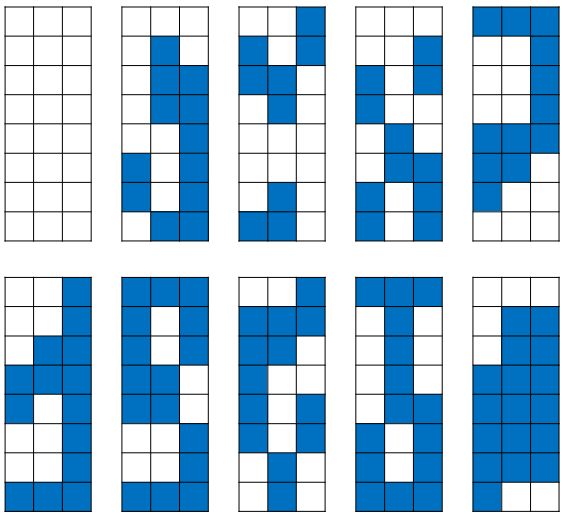

FIGURE 5. 15/24 non-ITI codewords with an MHD of 3.

second types. However, we use patterns with a size of 3 × 8. In these patterns we only avoid ISI (non-ISI patterns) while allowing ITI, as shown in Fig. 6.

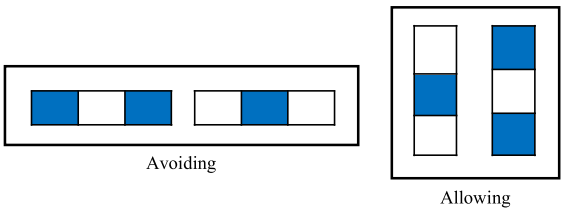

FIGURE 6. ISI patterns that we want to avoid.

To create the patterns of the third type, we reused the patterns of the second type by rotating these patterns by 90° as in Fig. 7.

IV. SIMULATION RESULTS

In this section, we utilized the diagram presented in Fig. 8 to simulate our proposed model. During simulation, we generated the user data $u[k]$ with a length of 1,440,000 bits, with an equal probability of occurrence for both '1' and '0' bits. After encoding, the user data $u[k]$ was converted to 2D data $c_{2D}[j,k] \in \{-1,1\}$ with a size of 1200 × 1200, representing a page.

The signal $c_{2D}[j,k]$ was then transmitted through the BPMR channel. The output of the BPMR channel was fed into the equalizer and detected by the soft-output Viterbi algorithm (SOVA) as described in [13], resulting in the creation of the signal $\hat{c}_{2D}[j,k]$. Finally, the signal $\hat{c}_{2D}[j,k]$ was used to decode the original signal $\hat{u}[k]$.

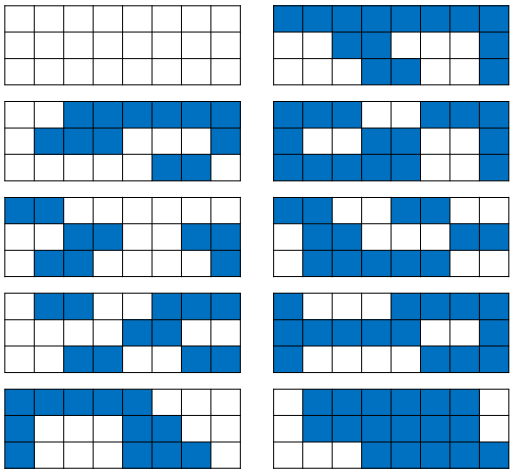

FIGURE 7. 15/24 non-ISI codewords with an MHD of 3.

In this study, we employed a page for estimating the parameters of the equalizer and target using the minimum mean square error (MMSE) algorithm as described in [3]. We utilized 10 pages to calculate the bit error rate (BER) performance of the system. The signal-to-noise ratio (SNR) was defined as follows.

$$\mathrm{SNR} = 10\log\left(1/\sigma^2\right). \tag{8}$$

In addition, the parameters of the simulation environment and model channel are presented in Table 1.

TABLE 1. The parameters of the simulation environment and model channel.

Parameters	Values
Central Processing Unit	Core i5-11400
Memory	24 GB
Graphics Processing Unit	GTX 1650
PW_x	19.4 nm
PW_q	24.8 nm
μ	1/2.3548
ε	0.9

In the first experiment, the BER performances of the three types 15/24 modulation codes are presented in Fig. 10. From these results, it is evident that the non-ITI modulation code achieves the best performance. This can be attributed to the fact that ITI is more detrimental than ISI. Furthermore, since the non-isolated patterns can include the ITI patterns, the non-ITI modulation outperforms both the non-isolated and non-ISI patterns. In addition, we also simulate the 15/24 non-isolated modulation code with the size of 6 × 4 in Fig. 9. These patterns in Fig. 9 are the 90° rotation of the patterns in Fig. 3.

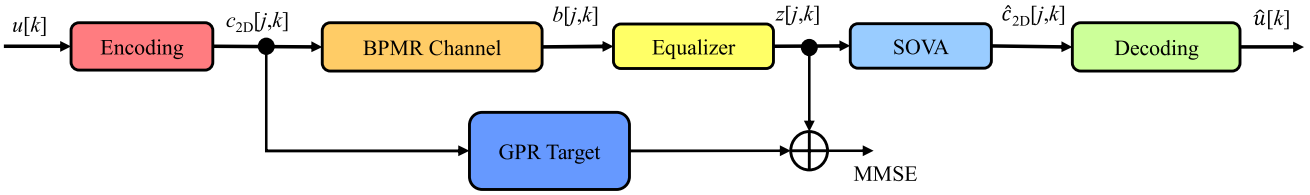

FIGURE 8. Diagram of model simulation.

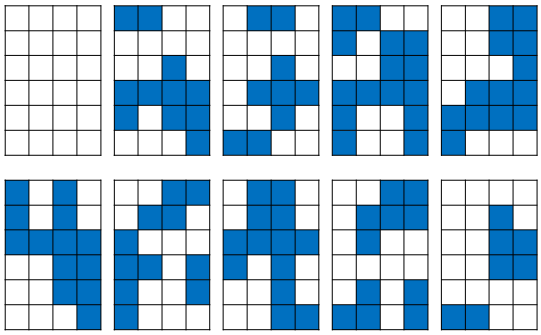

FIGURE 9. 15/24 non-isolated codewords with an MHD of 3 with 6 × 4.

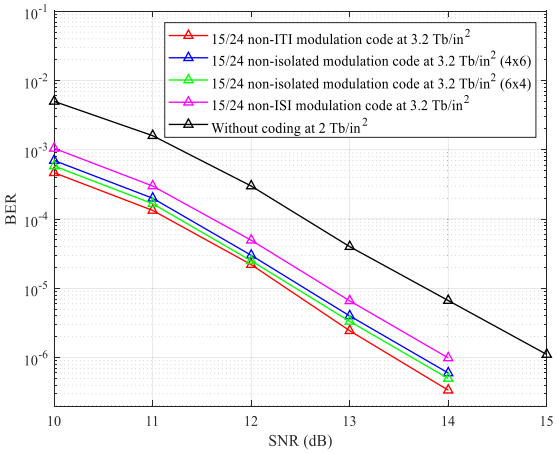

FIGURE 10. BER performance of three types of the 15/24 modulation codes.

In the second experiment, we compared our proposed model with the model presented in [12]. The results are depicted in Fig. 11. To maintain the length of user data, we simulate the 15/24 modulation code at an AD of 3.2 Tb/in^2 ($T_x = T_q = 14$ nm), the 20/30 modulation code at an AD of 3 Tb/in^2 ($T_x = T_q = 14.5$ nm), the 5/6 non-ITI modulation at an AD of 2.4 Tb/in^2 ($T_x = T_q = 16.4$ nm), the 4/6 modulation code at an AD of 3 Tb/in^2 ($T_x = T_q = 14.5$ nm), the 8/9 modulation code at an AD of 2.25 Tb/in^2 ($T_x = T_q = 16.74$ nm), the 9/12 modulation code at an AD of 2.6 Tb/in^2 ($T_x = T_q = 15.5$ nm), and the model without coding at an AD of 2 Tb/in^2($T_x = T_q = 18$ nm). For the 5/6 non-ITI modulation, we utilized the codewords presented in [15]. For the 4/6, 8/9, and 9/12 modulation codes, we used the codewords in [11], [16], and [17], respectively. We can see that our proposed code with MHD of 3 can achieve the better performance than the codes in [11], [16], and [17] with MHD of 2.

It can be observed that our proposed model improves the BER performance compared to the previous model. At a BER of 10^{-5}, our proposed code achieves a gain of 0.2 dB and 2 dB compared to the model in [12] and the model without coding, respectively. Typically, to improve the BER performance of BPMR systems, coding techniques often include codewords that avoid isolated patterns, particularly focusing on non-ITI patterns. However, in this paper, we propose a coding scheme that incorporates two key factors: non-ITI patterns and a minimum Hamming distance of 3. This combination enhances BER performance more effectively than previous studies. Additionally, our proposed 15/24 coding, which has fewer codewords than the 20/30 non-isolated modulation code, simplifies the detection process between the received signal and codewords. As a result, our 15/24 coding achieves better BER performance than the 20/30 modulation code.

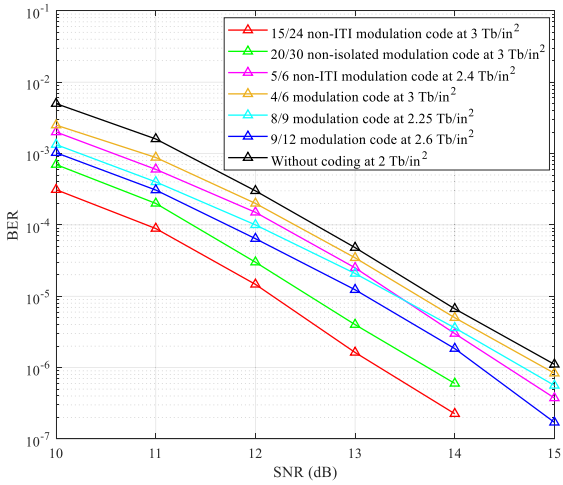

FIGURE 11. Comparison of the proposed code and previous studies.

Simultaneously, we measured the time for encoding and decoding, as shown in Table 2. We can see that our proposed model can reduce the time required by almost half compared to the previous model. In Table 2, the preserve the number of the codewords, we implemented our method in this paper to find out the codewords for 20/30 modulation code. Simultaneously, we also apply the method in [12] to find out the codewords for 15/24 modulation code.

TABLE 2. Time consumed by encoder and decoder for two methods.

	Encoder	Decoder
Method in [12] for 20/30 modulation code	2.26s	1061.02s
Method in [12] for 15/24 modulation code	1.37s	870.4s
Proposed method for 20/30 modulation code	2.14s	667.8s
Proposed method for 15/24 modulation code	1.43s	507.6s

s: second.

For the complexity of the proposed model, we count the number of operators when decoding a bit. Since our decoder uses the mapping algorithm in [12], the number of operators is equal to the number of the comparisons between the received signal and the codewords. For our proposed model, the codeword list is reduced by half compared to the codeword list in [12] because our proposed model adds the reverse bit processing. In MATLAB, the time to reverse the bit sequence is equivalent to the time of one or two addition operations, depending on the length of the bit sequence. Therefore, with the reverse bit processing, we count two addition operations. The results are presented in Table 3.

TABLE 3. The number of operators in decoder.

	Sub/Add	Mul/Div
Method in [12] for 20/30 modulation code	2097152	1048576
Method in [12] for 15/24 modulation code	65536	32768
Proposed method for 20/30 modulation code	1048577	524288
Proposed method for 15/24 modulation code	32769	16384
4/6 modulation code	32	16
8/9 modulation code	512	256
9/12 modulation code	1024	512

In the next experiments, to evaluate our proposed model in a more realistic environment, we introduced the TMR effect and media noise into the BPMR channel. Firstly, the TMR effect was incorporated into the BPMR channel. We fixed the SNR at 13 dB, while the TMR value was varied within the range of 10% to 30%. The results are depicted in Fig. 12. Our proposed model exhibited enhancements in the BER performance of BPMR systems by leveraging the TMR effect. Additionally, our proposed model demonstrated resilience to the TMR effect at values lower than 25%.

In the next experiment, we introduced media noise to the BPMR channel, considering the effects of position fluctuation. The results are illustrated in Fig. 13. We varied the position fluctuation levels from 6 to 18%, while keeping the SNR fixed at 13 dB. It was observed that when the position fluctuation level reached 14%, there was no notable difference in the BER performance across all tested methods.

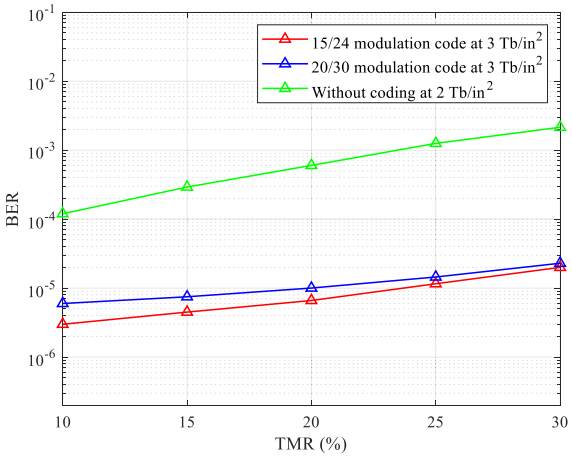

FIGURE 12. BER performances based on TMR at SNR = 13 dB.

Hence, it can be inferred that our proposed model demonstrates resilience against position fluctuations of up to 14%.

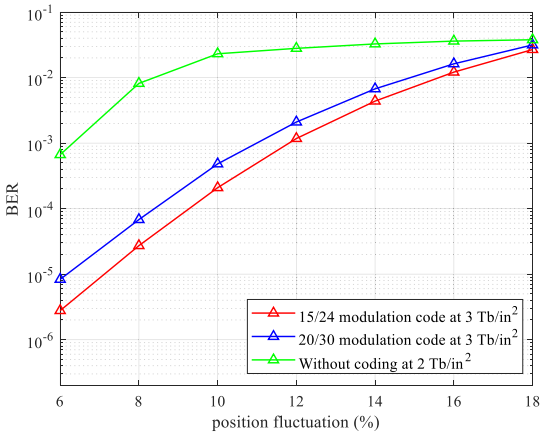

FIGURE 13. BER performances according to the position fluctuation.

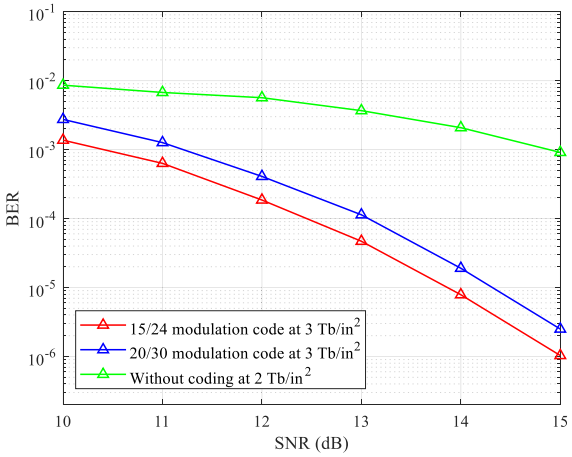

FIGURE 14. BER performances with 10% TMR effect and 6% position fluctuation.

Finally, we introduced both TMR and media noise to the BPMR channel. The BER performance of the proposed method is depicted in Fig. 14. We applied 6% position

fluctuation and 10% TMR to the BPMR channel. Additionally, we varied the SNR from 10 to 15 dB. The results show that the proposed model achieved the best performance under these conditions.

V. CONCLUSION

In this study, we propose a method that facilitates the creation of reverse codewords for non-isolated patterned modulation code with an MHD of 3. As a result, our proposed model reduces time consumption by half compared to the previous study. This method is based on the parity matrix of the Hamming code. When the number of '1's in each column of the parity matrix is odd, the codewords derived from this parity matrix will exist as inverses of each other. Simulation results demonstrate that the proposed code can enhance the BER performance of BPMR systems. Moreover, the proposed model exhibits resilience against TMR and position fluctuations of up to 25% and 14%, respectively. Even when both the TMR effect and media noise are considered, the codewords presented in our proposal maintain optimal performance.

APPENDIX

In Section III, we presented that if the number of '1's in each column of matrix $\mathbf{P}$ is odd or the summation of each column in the matrix is 1, the codewords c_{2D} always have the reversed binary sequence. In this section, we will prove this issue.

We have defined the codeword as shown below:

$$\begin{aligned}\mathbf{c}^T &= \left[\, a_0\ a_1\ a_2\ \ldots\ a_{2^s-s-3} \,\middle|\, p_0\ p_1\ p_2\ \ldots\ p_{s-1} \,\right] \\ &= \left[\, \mathbf{a}^T \,\middle|\, \mathbf{p}^T \,\right] \\ &= \left[\, a_0\ a_1\ a_2\ \ldots\ a_{2^s-s-3} \,\right] \mathbf{G} \\ &= \left[\, a_0\ a_1\ a_2\ \ldots\ a_{2^s-s-3} \,\right] [\mathbf{I}|\,\mathbf{P}]\,. \end{aligned} \tag{9}$$

The value of $\bar{\mathbf{c}}$ can be deduced as shown below.

$$\bar{\mathbf{c}}^T = \left[\, \bar{\mathbf{a}}^T \,\middle|\, \bar{\mathbf{p}}^T \,\right]. \tag{10}$$

The parity matrix $\mathbf{P}$ is presented below.

$$\mathbf{P} = \begin{bmatrix} t_{0,0} & t_{0,1} & t_{0,2} & \cdots & t_{0,s-1} \\ t_{1,0} & t_{1,1} & t_{1,2} & \cdots & t_{1,s-1} \\ t_{2,0} & t_{2,1} & t_{2,2} & \cdots & t_{2,s-1} \\ \vdots & \vdots & \vdots & \ddots & \vdots \\ t_{r-1,0} & t_{r-1,1} & t_{r-1,2} & \cdots & t_{r-1,s-1} \end{bmatrix}. \tag{11}$$

Using the provided definitions of $\mathbf{a}$, $\mathbf{p}$, and $\mathbf{P}$, the calculation of $\mathbf{p}$ is as follows.

$$\mathbf{p}^T = \mathbf{a}^T\mathbf{P}$$

with

$$\mathbf{p}^T = \left[\, p_0\ p_1\ p_2\ \cdots\ p_{s-1} \,\right]$$

$$\mathbf{a}^T = \left[\, a_0\ a_1\ a_2\ \ldots\ a_{s-1} \,\right]$$

$$\mathbf{P} = \begin{bmatrix} t_{0,0} & t_{0,1} & t_{0,2} & \cdots & t_{0,s-1} \\ t_{1,0} & t_{1,1} & t_{1,2} & \cdots & t_{1,s-1} \\ t_{2,0} & t_{2,1} & t_{2,2} & \cdots & t_{2,s-1} \\ \vdots & \vdots & \vdots & \ddots & \vdots \\ t_{r-1,0} & t_{r-1,1} & t_{r-1,2} & \cdots & t_{r-1,s-1} \end{bmatrix}. \tag{12}$$

We can rewrite the equation (12) as below.

$$\begin{cases} p_0 = a_0t_{0,0} + a_1t_{1,0} + a_2t_{2,0} + \ldots + a_{r-1}t_{r-1,0} \\ p_1 = a_1t_{0,1} + a_1t_{1,1} + a_2t_{2,1} + \ldots + a_{r-1}t_{r-1,1} \\ \vdots \\ p_{s-1} = a_1t_{0,s-1} + a_1t_{1,s-1} + a_2t_{2,s-1} \\ \qquad + \ldots + a_{r-1}t_{r-1,s-1}. \end{cases} \tag{13}$$

If we replace $\mathbf{a}$ with $\bar{\mathbf{a}}$, we will obtain the below equation:

$$\begin{cases} p_0^{\bar{\mathbf{a}}} = \bar{a}_0t_{0,0} + \bar{a}_1t_{1,0} + \bar{a}_2t_{2,0} + \ldots + \bar{a}_{r-1}t_{r-1,0} \\ p_1^{\bar{\mathbf{a}}} = \bar{a}_1t_{0,1} + \bar{a}_1t_{1,1} + \bar{a}_2t_{2,1} + \ldots + \bar{a}_{r-1}t_{r-1,1} \\ \vdots \\ p_{s-1}^{\bar{\mathbf{a}}} = \bar{a}_1t_{0,s-1} + \bar{a}_1t_{1,s-1} + \bar{a}_2t_{2,s-1} \\ \qquad + \ldots + \bar{a}_{r-1}t_{r-1,s-1}. \end{cases} \tag{14}$$

where $\mathbf{c}^{\bar{a}} = [\bar{\mathbf{a}}|\mathbf{p}^{\bar{a}}]$. We add the equations (13) and (14) as below.

$$\begin{cases} p_0 + p_0^{\bar{\mathbf{a}}} = t_{0,0} + t_{1,0} + t_{2,0} + \ldots + t_{r-1,0} = 1 \\ p_1 + p_1^{\bar{\mathbf{a}}} = t_{0,1} + t_{1,1} + t_{2,1} + \ldots + t_{r-1,1} = 1 \\ \vdots \\ p_{s-1} + p_{s-1}^{\bar{\mathbf{a}}} = t_{0,s-1} + t_{1,s-1} + t_{2,s-1} \\ \qquad + \ldots + t_{r-1,s-1} = 1. \end{cases} \tag{15}$$

From (15), we deduce the below expression.

$$\mathbf{p} + \mathbf{p}^{\bar{\mathbf{a}}} = \mathbf{1}. \tag{16}$$

where $\mathbf{1} = [1\ 1\ 1\ 1\ \ldots 1]$. Thus,

$$\mathbf{p}^{\bar{\mathbf{a}}} = \bar{\mathbf{p}}. \tag{17}$$

Then,

$$\mathbf{c}^{\bar{\mathbf{a}}} = \left[\, \bar{\mathbf{a}} \,\middle|\, \mathbf{p}^{\bar{\mathbf{a}}} \,\right] = [\,\bar{\mathbf{a}}|\,\bar{\mathbf{p}}] = \bar{\mathbf{c}}. \tag{18}$$

Therefore, the codeword list always includes the reversed codewords because all cases of vector $\mathbf{a}$ always have the reversed sequences.

REFERENCES

[1] S. Nabavi, B. V. K. V. Kumar, and J. A. Bain, "Two-dimensional pulse response and media noise modeling for bit-patterned media," *IEEE Trans. Magn.*, vol. 44, no. 11, pp. 3789–3792, Nov. 2008.

[2] S. Jeong and J. Lee, "Track mis-registration estimator based on K-means algorithm for bit-patterned media recording," *IEEE Trans. Magn.*, vol. 59, no. 3, pp. 1–5, Mar. 2023.

[3] S. Nabavi and B. V. K. V. Kumar, "Two-dimensional generalized partial response equalizer for bit-patterned media," in *Proc. IEEE Int. Conf. Commun.*, Jun. 2007, pp. 6249–6254.

[4] R. D. Cideciyan, F. Dolivo, R. Hermann, W. Hirt, and W. Schott, "A PRML system for digital magnetic recording," *IEEE J. Sel. Areas Commun.*, vol. 10, no. 1, pp. 38–56, Jan. 1992.

[5] Y. Wang and B. V. K. V. Kumar, "Improved multitrack detection with hybrid 2-D equalizer and modified Viterbi detector," *IEEE Trans. Magn.*, vol. 53, no. 10, pp. 1–10, Oct. 2017.

[6] S. Nabavi, B. V. K. V. Kumar, and J.-G. Zhu, "Modifying Viterbi algorithm to mitigate intertrack interference in bit-patterned media," *IEEE Trans. Magn.*, vol. 43, no. 6, pp. 2274–2276, Jun. 2007.

[7] S. Jeong and J. Lee, "Soft-output detector using multi-layer perceptron for bit-patterned media recording," *Appl. Sci.*, vol. 12, no. 2, p. 620, Jan. 2022.

[8] A. Sayyafan, A. Aboutaleb, B. J. Belzer, K. Sivakumar, A. Aguilar, C. A. Pinkham, K. S. Chan, and A. James, "Deep neural network media noise predictor turbo-detection system for 1-D and 2-D high-density magnetic recording," *IEEE Trans. Magn.*, vol. 57, no. 3, pp. 1–13, Mar. 2021.
[9] K. Buahing, W. Busyatras, and C. Warisarn, "A rate-5/6 2D modulation code for single-reader/two-track reading in BPMR systems," in *Proc. IEEE Int. Magn. Conf. (INTERMAG)*, Apr. 2018, p. 1.
[10] T. A. Nguyen and J. Lee, "Error-correcting 5/6 modulation code for staggered bit-patterned media recording systems," *IEEE Magn. Lett.*, vol. 10, pp. 1–5, 2019.
[11] S. Jeong and J. Lee, "Modulation decoding based on K-means algorithm for bit-patterned media recording," *Appl. Sci.*, vol. 12, no. 17, p. 8703, Aug. 2022.
[12] T. A. Nguyen and J. Lee, "Design of non-isolated modulation code with minimum Hamming distance of 3 for bit-patterned media-recording systems," *IEEE Trans. Magn.*, vol. 59, no. 11, pp. 1–5, May 2023.
[13] S. Jeong, J. Kim, and J. Lee, "Performance of bit-patterned media recording according to island patterns," *IEEE Trans. Magn.*, vol. 54, no. 11, pp. 1–4, Nov. 2018.
[14] S. Nabavi, B. V. K. Vijaya Kumar, J. A. Bain, C. Hogg, and S. A. Majetich, "Application of image processing to characterize patterning noise in self-assembled nano-masks for bit-patterned media," *IEEE Trans. Magn.*, vol. 45, no. 10, pp. 3523–3526, Oct. 2009.
[15] C. Warisarn, A. Arrayangkool, and P. Kovintavewat, "An ITI-mitigating 5/6 modulation code for bit-patterned media recording," *IEICE Trans. Electron.*, vol. E98-C, no. 6, pp. 528–533, 2015.
[16] P. Kovintavewat, A. Arrayangkool, and C. Warisarn, "A rate-8/9 2-D modulation code for bit-patterned media recording," *IEEE Trans. Magn.*, vol. 50, no. 11, pp. 1–4, Nov. 2014.
[17] C. D. Nguyen and J. Lee, "Elimination of two-dimensional intersymbol interference through the use of a 9/12 two-dimensional modulation code," *IET Commun.*, vol. 10, no. 14, pp. 1–6, Sep. 2016.

THIEN AN NGUYEN received the Bachelor of Engineering degree in electronics-telecommunications engineering from the Ho Chi Minh University of Technology, Vietnam, in 2018. He is currently pursuing the Ph.D. degree with Soongsil University, Seoul, South Korea. His research interests include signal processing and detection algorithms, error-correction codes, and modulation codes.

JAEJIN LEE (Member, IEEE) received the B.S. degree from Yonsei University, Seoul, South Korea, in 1983, the M.S.E.E. degree from the University of Michigan, Ann Arbor, MI, USA, in 1984, and the Ph.D. degree from Georgia Institute of Technology, Atlanta, GA, USA, in 1994. He has been working on DVD systems as a Senior Engineer with the IT Research and Development, Hyundai Electronics Industries Company Ltd. From March 1997 to August 2005, he was with Dongguk University. In September 2005, he joined the School of Electronic Engineering, Soongsil University, Seoul. His research interests include signal processing and coding for storage and communication systems.